To cite this document: GOIFFON Vincent, MAGNAN Pierre, MARTIN-GONTHIER Philippe, VIRMONTOIS Cédric and GAILLARDIN Marc. New source of random telegraph signal in CMOS image sensors. In: *International Image Sensor Workshop*, 08-11 June 2011, Hakodate-Onuma Prince Hotel, Hokaido, Japan.

New Source of Random Telegraph Signal in CMOS Image Sensors

V. Goiffon, P. Magnan, P. Martin-Gonthier, C. Virmontois, and M. Gaillardin

RANDOM TELEGRAPH SIGNAL (RTS) can define two distinct phenomena in CMOS Image Sensors (CIS), as illustrated in Fig. 1. The first is a temporal noise source contributing to the sensor readout noise due to the discrete fluctuation of the in-pixel source follower (SF) channel conductance [1]. This well known phenomenon in small geometry MOSFET [2], is due to the trapping and emission of channel carriers by oxide traps and will be called MOSFET-RTS in this paper.

The second type is a discrete variation of the photodiode Dark Current (DC) and will be called DC-RTS in the following. Two sources have been reported so far for DC-RTS in CIS (also shown in Fig. 1). The first one has been attributed to displacement damage induced meta-stable Recombination/Generation (R-G) centers located in the depleted volume of CCDs and CISs [3]–[6]. It was clearly shown in early studies [3]–[6] that ionizing radiation (^{60}Co γ-rays) did not induce such DC-RTS in CCDs and in LOCOS-based CISs, leading to the conclusion that this DC-RTS was not due to oxide defects but to bulk damages only. A second source of DC-RTS has been reported at least once [7] in CIS manufactured with a $0.15\ \mu$m CMOS process, not optimized for imaging application where high electric fields exist in the vicinity of the reset MOSFET gate. The reported DC-RTSs were extremely dependent on electric field and photodiode bias. They were thus attributed to trap assisted tunneling at the reset MOSFET gate oxide interface. TAT induced DC-RTS is not likely to happen in sensors manufactured using CMOS process dedicated to imaging, since electric fields are optimized in such sensors to avoid TAT and electric field enhanced dark current sources.

In this workshop proceeding paper, we present a new source of DC-RTS [8] due to meta-stable Shockley-Read-Hall (SRH) generation mechanism at depleted oxide interfaces (also observed in DRAMs [9] and in bipolar transistors [10]). This DC-RTS is very similar to displacement damage DC-RTS except that it is due to meta-stable oxide R-G centers instead of meta-stable bulk generation centers.

The studied CIS are $10\ \mu$m-pitch 128×128-pixel arrays with 3T-pixels and manufactured using a 3.3 V commercial $0.18\ \mu$m CIS process. To reveal the DC-RTS phenomenon, dark frames were acquired at a regular sampling rate and fixed integration time (typically 1 s) for a few hours at stabilized temperature 22°C.

V. Goiffon, P. Magnan, P. Martin-Gonthier and C. Virmontois are with Université de Toulouse, ISAE, Toulouse F-31055, France.

M. Gaillardin is with CEA DAM, DIF F-91297 Arpajon, France.

I. MOSFET-RTS AND DC-RTS DISCRIMINATION

The studied sensors exhibited random discrete signal fluctuations in the dark. Before studying these fluctuations further, it is important to clarify the differences between MOSFET-RTS and DC-RTS. These two phenomena are very different in nature and so are their effects. MOSFET-RTS in an N-channel transistor is caused by an oxide (gate and/or STI) electron trap [2]. When the semiconductor under the gate is inverted, this trap can capture and emit a channel electron. When a charge carrier is trapped, the MOST channel conductance is instantaneously reduced. When this electron is emitted, the channel conductance goes back to its original value leading to a discrete fluctuation of the transconductance. That is the reason why the time constant of the high conductance state (i.e. high current state) is called the capture time constant, whereas the low conductance state (i.e. low current state) time constant is named the emission time constant [2]. MOSFET-RTS is only visible in CIS when the MOSFET channel conductance changes between the reference and the signal samples. Thus, if the time constant of the capture/emission process is shorter than the inter-sample time (reference sample and signal sample of the same frame), this discrete source follower transconductance fluctuation can generate an additional temporal noise contribution to the readout noise. If the MOSFET-RTS is slower than the inter-sample time, it will not have any influence on CIS performances.

DC-RTS is not due to traps[1] but to SRH R-G centers. The R-G centers causing DC-RTS are meta-stable and their generation rate change instantaneously and randomly with time leading to discrete leakage current fluctuations in PN junctions. Electrons are continuously passing through RTS R-G centers (continuous emission of electrons and holes), as any R-G centers in a depleted region. The high and low current states correspond to a defect configuration inducing respectively a high and low generation rate. It has never been shown so far, to our knowledge, that these high and low generation sates of a DC-RTS center are related to the emission and capture of a charge carrier. Thus, the concept of emission time constant

[1]Except TAT-DC-RTS which is a very particular and unusual case.

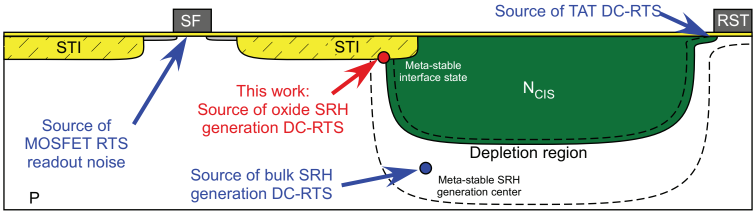

Fig. 1. Illustration of the different origins of CIS RTS. The new source of RTS reported here is shown in red.

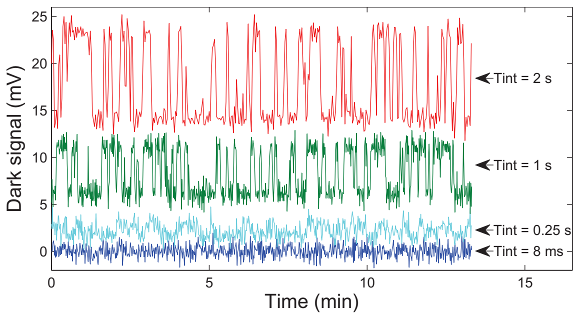

Fig. 2. Influence of the integration time on the studied RTS behavior clearly showing that the observed RTS are DC-RTS.

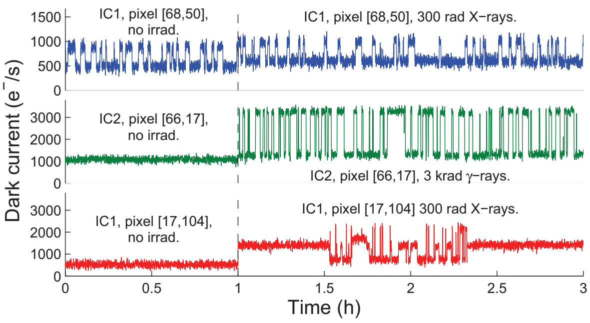

Fig. 3. Temporal representation of a selection of typical DC-RTS.

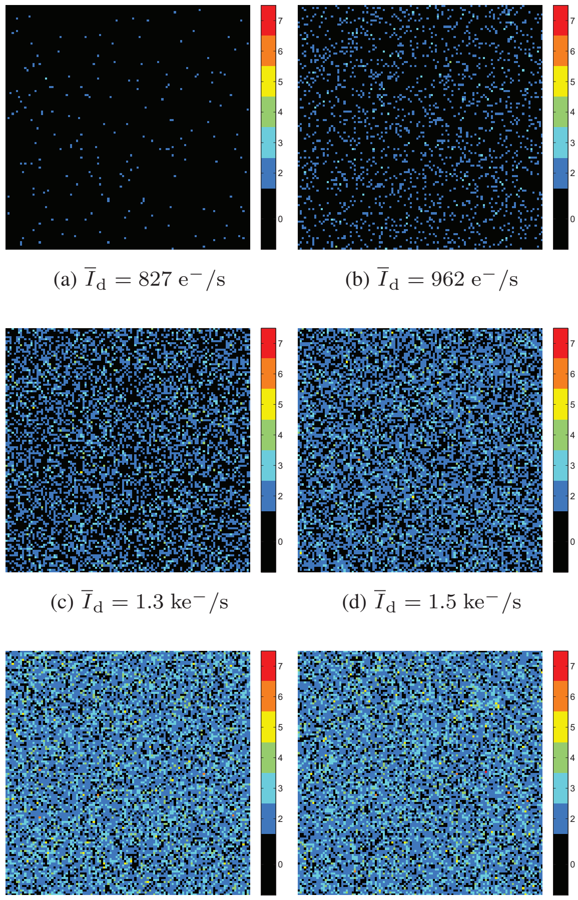

(a) $\overline{I}_{\mathrm{d}} = 827\ \mathrm{e}^{-}/\mathrm{s}$ (b) $\overline{I}_{\mathrm{d}} = 962\ \mathrm{e}^{-}/\mathrm{s}$

(c) $\overline{I}_{\mathrm{d}} = 1.3\ \mathrm{ke}^{-}/\mathrm{s}$ (d) $\overline{I}_{\mathrm{d}} = 1.5\ \mathrm{ke}^{-}/\mathrm{s}$

(e) $\overline{I}_{\mathrm{d}} = 2.7\ \mathrm{ke}^{-}/\mathrm{s}$ (f) $\overline{I}_{\mathrm{d}} = 5.4\ \mathrm{ke}^{-}/\mathrm{s}$

Fig. 4. Mappings of the number of detected RTS levels (indicated by the colorbar) per pixel for several TID: (a) IC1 before irradiation, (b) IC1 300 rad, (c) IC1 1 krad, (d) IC2 3 krad, (e) IC2 10 krad, (f) IC2 30 krad . Integration time = 1 s , sampling time = 2 s, measurement duration 12 h, temperature = 22°C. The mean dark current $\overline{I}_{\mathrm{d}}$ value after each irradiation is indicated under each figure.

and capture time constant can not be applied to leakage current RTS. The consequence of DC-RTS on CIS performances is a discrete fluctuation of dark current from one frame to another.

The most straightforward way to discriminate the two effects in an image sensor, is to see whether the RTS amplitude is proportional to integration time or not. Fig. 2 shows an example of the evolution of amplitude of the RTS studied in this paper as a function of integration time. It can clearly be seen that this RTS amplitude is directly proportional to the integration time leading to the conclusion that this RTS is a DC-RTS. One can also notice that the RTS time constants shown in this paper are much longer than the inter-sample time ($\approx 2\ \mu$s), and can therefore not be due to MOSFET-RTS.

II. Origin of the observed DC-RTS

In order to reveal the origin of the observed DC-RTSs, ionizing radiation sources (X-rays and ^{60}Co gamma rays) were used to generate only oxide defects[2]. The dark current evolution as a function of time of a selection of pixels is presented in Fig. 3 before and after exposure to ionizing radiation. It can clearly be seen that, in addition to an increase of the dark current pedestal due to the buildup of stable interface R-G centers, large discrete dark current fluctuations appear after exposure to ionizing radiation in pixels

[2]The probability for ^{60}Co gamma rays to generate bulk defects is not zero. However, this probability is extremely small in comparison to the oxide defect densities generated by such sources in CMOS circuits.

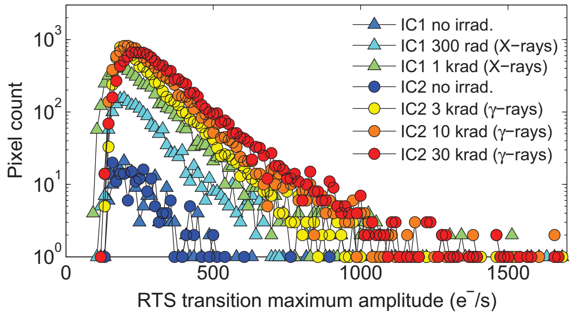

Fig. 5. RTS maximum transition amplitude distribution for several TID (same test conditions as Fig. 4). Extreme values go up to $2700\ e^{-}/s$.

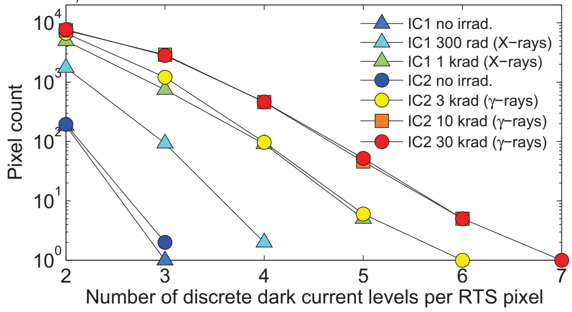

Fig. 6. Distribution of the number of discrete switching levels per RTS pixel as a function of TID (same test conditions as Fig. 4).

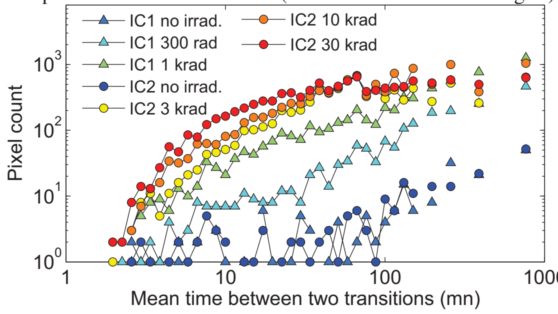

Fig. 7. Distribution of the mean time between two RTS transitions as a function of TID (same test conditions as Fig. 4).

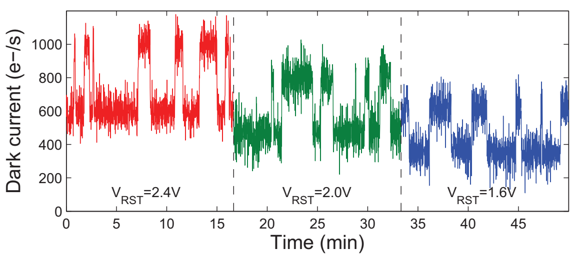

Fig. 8. Influence of the photodiode (hard) reset bias on the RTS amplitude.

[66,17] and [17,104]. These DC-RTSs generated by the ionizing particles were very similar in the temporal domain to the DC-RTSs already existing in the unirradiated devices (such as the one of pixel [68,50]).

The mappings of detected RTSs before and after exposure to X and γ-rays are presented in Fig. 4. A

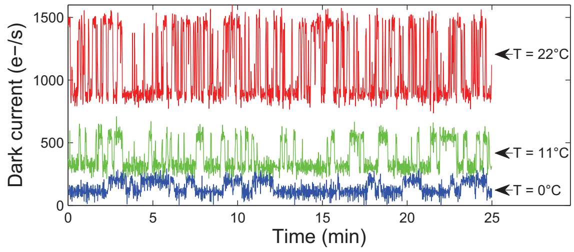

Fig. 9. Influence of the temperature on the RTS behavior. RTS amplitude $E_{\rm act} = 0.59$ eV. Dark current pedestal $E_{\rm act} = 0.64$ eV.

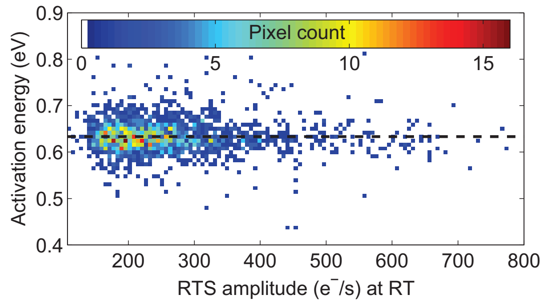

Fig. 10. RTS pixels dark current activation energy distribution as a function of maximum RTS transition amplitude at 22°C after 300 rad.

significant number of RTS pixels are detected[3] before irradiation but this number rises clearly with Total Ionizing Dose (TID)[4] indicating that oxide defects are responsible. One can notice on the pixel [17,104] dark current plot (Fig. 3) that the observed DC-RTS can be non-stationary, and that a single RTS defect can lead to more than two dark current discrete levels (as in the case of bulk defect DC-RTS [12]).

The distributions of the maximum RTS transition amplitudes detected per RTS pixel is presented in Fig. 5. The right part of the distributions is exponentially distributed, with a similar slope for every distribution in this semilogarithmic plot[5]. The fact that this slope is not changing significantly with TID, and especially that the slope is the same before and after exposure to radiation, strongly suggests that the DC-RTSs observed before irradiation are similar to those generated by the ionizing particles.

Fig. 6 shows that the number of DC-RTS levels also rises with TID. This is explained by the increasing probability (with TID) of having several two-level-RTS centers in a single pixel and also by the generation of some multi-level RTS centers (such as in the pixel [17,104] dark current in Fig. 3). As regards the observed RTS time constants presented in Fig. 7, they cover the entire detection range: from a few time the detection filter length (≈ 1 mn) up to the measurement

[3]The details of the detection method can be found in [11].

[4]Radiation doses are given in rad(SiO_2).

[5]The fact that this exponential distribution does not extend below $200\ e^{-}/s$ is due to the noise background which limit the detection efficiency at low RTS amplitude values.

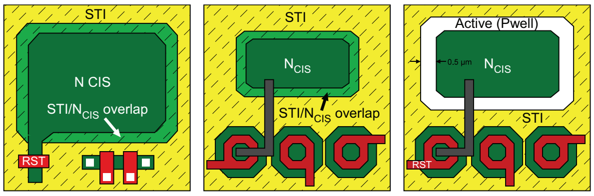

(a) (b) (c)

Fig. 11. Layout illustration (not to scale) of the three types of studied pixels. (a) Standard pixel layout used for the previous figures. (b) Pixel with enclosed layout transistors and a standard photodiode. (c) Pixel with enclosed layout transistors and a photodiode with recessed field oxide (0.5 μm away from the junction). Photodiodes of pixel (b) and (c) have the same junction perimeter and area.

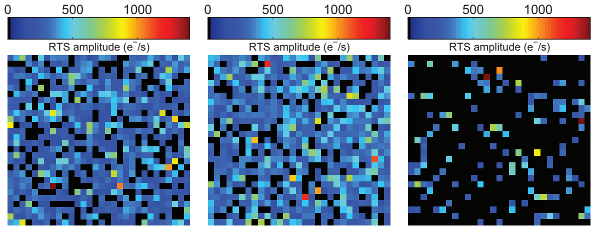

(a) (b) (c)

Fig. 12. Mappings of detected RTS pixels amplitudes after 30 krad for the three studied pixel layouts: (a) standard, (b) standard with ELT in-pixel MOSFETs, (c) recessed field oxide and ELT in-pixel MOSFETs.

duration (several hours). It is therefore very likely that the physical process at the origin of this DC-RTS can be much faster (and also much slower) than what is seen through this temporal detection window.

The evolution of a typical DC-RTS with photodiode reset voltage is presented in Fig. 8. It can clearly be seen that the DC-RTS amplitude is very weakly dependent on the photodiode reverse bias. Hence, it can be inferred that this kind of DC-RTS is not dominated by an electric field dependent contribution in contrary to what was observed in TAT DC-RTS [7]. This is confirmed by the DC-RTS amplitude activation energy around 0.6 eV (e.g. Fig. 9 and Fig. 10) and the mean dark current activation energy ($E_{\mathrm{act}} = 0.63 \pm 0.03$ eV on the whole irradiated array), both around the midgap value, typical for SRH generation currents in depleted regions.

In order to localize more precisely the oxide mainly responsible for this RTS, another pixel array manufactured on the same die with the same layout except that the STI has been drawn 0.5 μm away from the photodiode junction (Fig. 11) has been irradiated. As can be seen in 12, recessing the STI 0.5 μm away from the photodiode junction leads to a reduction of more than 75% of the number of detected RTS pixels. This last observation strongly suggests that the STI is the main contributor to the reported RTS. The remaining RTS in the recessed oxide photodiode most likely comes from the oxide interface located just above the photodiode.

III. Summary and Conclusion

We reported discrete dark current fluctuations in CIS attributed to meta-stable oxide SRH R-G centers located in the photodiode depletion region, mainly coming from the STI depleted interfaces. The number of such DC-RTSs rose significantly with the exposure to ionizing radiation. The large number of RTS pixels generated at fairly low total ionizing dose implies that this novel source of DC-RTS can be an important issue for CISs operated in ionizing environments (space, nuclear, scientific, military...). The few RTS pixels existing in non-irradiated devices may also be a concern in some low light level applications. Such R-G current RTS is likely to appear in any reverse biased PN junction where the depleted region touches an oxide interface. Analysis of oxide DC-RTS in CIS can also help to understand similar RTS behaviors in other devices, such as the variable retention time phenomenon in DRAMs. Finally, this RTS is clearly at the origin of the unexplained peak, at low amplitude, that was observed in proton irradiated CIS RTS amplitude distributions [11].

References

[1] C. Leyris, F. Martinez, M. Valenza, A. Hoffmann, J. Vildeuil, and F. Roy, "Impact of random telegraph signal in CMOS image sensors for low-light levels," in *Proc. ESSCIRC*, 2006, pp. 376–379.

[2] M. J. Kirton and M. J. Uren, "Noise in solid-state microstructures: A new perspective on individual defects, interface states and low-frequency (1/f) noise," *Adv. Phys.*, vol. 38, no. 4, pp. 367–468, 1989.

[3] I. H. Hopkins and G. R. Hopkinson, "Random telegraph signals from proton-irradiated CCDs," *IEEE Trans. Nucl. Sci.*, vol. 40, no. 6, pp. 1567–1574, Dec. 1993.

[4] ——, "Further measurements of random telegraph signals in proton-irradiated CCDs," *IEEE Trans. Nucl. Sci.*, vol. 42, no. 6, pp. 2074–2081, 1995.

[5] G. R. Hopkinson, "Radiation effects in a CMOS active pixel sensor," *IEEE Trans. Nucl. Sci.*, vol. 47, no. 6, pp. 2480–2484, Dec. 2000.

[6] J. Bogaerts, B. Dierickx, and R. Mertens, "Random telegraph signal in a radiation-hardened CMOS active pixel sensor," *IEEE Trans. Nucl. Sci.*, vol. 49, no. 1, pp. 249–257, Feb. 2002.

[7] B. Pain, B. Hancock, C. Sun, and C. Wrigley, "Twinkling pixels: Random telegraph signals at reset gate edge," in *Proc. Int. Image Sensor Workshop*, 2007, pp. 234–237.

[8] V. Goiffon, P. Magnan, P. Martin-Gonthier, C. Virmontois, and M. Gaillardin, "Evidence of a novel source of random telegraph signal in CMOS image sensors," *IEEE Electron Device Lett.*, vol. 32, no. 6, 2011.

[9] Y. Mori, K. Ohyu, K. Okonogi, and R. Yamada, "The origin of variable retention time in DRAM," in *IEEE IEDM Tech. Dig.*, Dec. 2005, pp. 1034–1037.

[10] D. Pogany, J. Chroboczek, and G. Ghibaudo, "Random telegraph signal noise mechanisms in reverse base current of hot carrier-degraded submicron bipolar transistors: Effect of carrier trapping during stress on noise characteristics," *J. Appl. Phys.*, vol. 89, p. 4049, 2001.

[11] V. Goiffon, G. R. Hopkinson, P. Magnan, F. Bernard, G. Rolland, and O. Saint-Pe, "Multilevel RTS in proton irradiated CMOS image sensors manufactured in a deep submicron technology," *IEEE Trans. Nucl. Sci.*, vol. 56, no. 4, pp. 2132–2141, Aug. 2009.

[12] G. R. Hopkinson, V. Goiffon, and A. Mohammadzadeh, "Random telegraph signals in proton irradiated CCDs and APS," *IEEE Trans. Nucl. Sci.*, vol. 55, no. 4, Aug. 2008.